Proceedings of the Twenty-Fourth AAAI Conference on Artificial Intelligence (AAAI-10)

Interactive Learning Using Manifold Geometry

Eric Eaton and **Gary Holness** and **Daniel McFarlane**
Lockheed Martin Advanced Technology Laboratories
Artificial Intelligence Research Group
3 Executive Campus, Suite 600; Cherry Hill, NJ 08002
{eeaton, gholness, dmcfarla}@atl.lmco.com

Abstract

We present an interactive learning method that enables a user to iteratively refine a regression model. The user examines the output of the model, visualized as the vertical axis of a 2D scatterplot, and provides corrections by repositioning individual data instances to the correct output level. Each repositioned data instance acts as a control point for altering the learned model, using the geometry underlying the data. We capture the underlying structure of the data as a manifold, on which we compute a set of basis functions as the foundation for learning. Our results show that manifold-based interactive learning improves performance monotonically with each correction, outperforming alternative approaches.

Introduction

Information management systems for high-volume applications, such as disease spread modeling and maritime situational awareness, monitor thousands of entities or events, only a small fraction of which are important to the user. In order to focus user attention, these systems typically assign a numeric score to each entity or event that represents its importance to the current situation as evaluated by a scoring function. In a typical system, the data is visualized as a 2D scatterplot (Figure 1), where the vertical axis depicts the score assigned to each data instance.

The scoring function is customized to the current situation. For example, a coastal monitoring system will have very different scoring functions depending on whether it is focused on surveillance or engaged in search and rescue operations. In many cases, there is no opportunity (or time) to obtain labeled data for a new situation, eliminating the possibility of using standard supervised approaches to learn a scoring function. Sets of predetermined "standard" models for each situation are a good starting place, but these models must still be manually tuned to match the current situation.

In many deployed applications, these scoring functions are manually specified to give the user fine control. This approach requires users to manually adjust a set of parameters to tune the scoring function—a procedure which is likely to be error prone for any sufficiently complex function. Additionally, this approach requires users to have detailed knowledge of the model parameters and their interactions. Therefore, these manually specified models tend to be relatively simple, such as rule-based statements, feature weights in linear functions, and other straightforward models that can be easily understood and specified by the average user. However, these simple scoring functions may be insufficient to capture a user's true intentions, such as bi-modal interests.

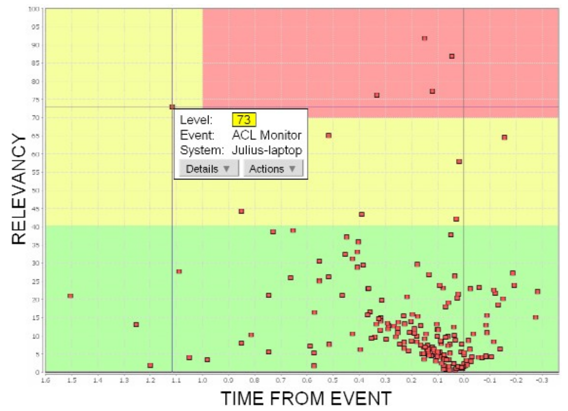

Figure 1: A 2D scatterplot representing the importance of events in a hypothetical network security system. The vertical axis depicts the score assigned to each event, quickly focusing user attention on the most important events.

We explore a novel method for interactively refining an initial scoring function using a combination of manual input and machine learning. The user first manually specifies a simple linear model as the starting point for learning. Users then examine the output of the model in the 2D scatterplot, and iteratively correct the model by repositioning data instances to the correct level. The system incorporates each correction into the learning process, using the manifold geometry underlying the data to determine the extent of each correction's effect on the learned model (Figure 2).

We project the data onto a set of basis functions defined by the manifold underlying the data, which can be computed automatically. Our approach learns using the manifold basis to ensure that each adjustment affects the model with respect to the natural geometry of the data. We use the basis-projected data in combination with the target scores to learn the scoring function using weighted least squares with Laplacian regularization. This learning method is a special

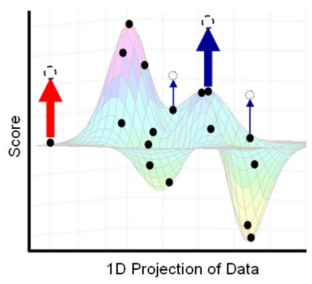

(a) User scatterplot view

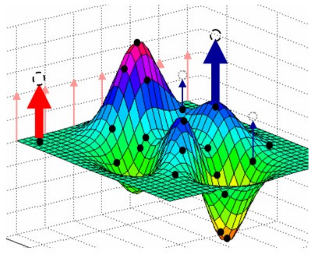

(b) Underlying manifold model

Figure 2: Interactive learning of a model, showing the user dragging two points (large light red and dark blue arrows) and the effect on the other data points and underlying scoring function. The red adjustment has a large effect due to the (geometrical) importance of this point, while the blue adjustment affects only points on the local peak.

case of Belkin et al.'s (2006) Manifold Regularization that constrains the smoothness of the learned function. Each successive change to the function updates the scatterplot, providing users with instantaneous feedback and allowing them to interactively refine the learned function. This interactive learning method enables the user to rapidly refine a simple initial scoring function to one of arbitrary complexity that captures their intentions. This approach requires that the user have general knowledge of the application domain, but it does not require knowledge of the model's internal structure. Results show that our interactive learning method monotonically improves performance with each correction, outperforming alternative approaches.

Mechanisms for User Interaction

Our approach is guided by the need for simplicity of interaction between the user and the data. Interactive mechanisms for learning should be intuitive and burden the user as little as possible while obtaining the feedback necessary to learn. Let the data be given by $X = \{\mathbf{x_i}\}_{i=1}^{n}$, where each data instance $\mathbf{x_i} \in \mathbb{R}^d$.

We assume that the system provides a 2D scatterplot of the data, where one axis (the vertical axis in this paper) depicts the value of each instance according to the scoring function. The other axis is a projection based either on the data (e.g., the first principal component) or determined by the user. Users can obtain a detailed view of a data instance's attributes to manually assess its score.

Initially, the user provides a simple function $\tilde{F} : \mathbb{R}^d \rightarrow [0, 1]$, such as a linear model, that is an approximation to the true (hidden) scoring function $F : \mathbb{R}^d \rightarrow [0, 1]$ intended by the user. The goal of interactive learning is to assist the user in correcting the simple function $\tilde{F}$ to match the true function F. Each instance's score is determined by the current scoring function f, which starts as $f = \tilde{F}$ and changes in response to the user's corrections, ideally until $f = F$.

The user provides corrections to the system by selecting a data instance and sliding it up or down along the vertical axis to correct its value (Figure 2). The adjusted value is then used to refine the learned function f. The ability to adjust the assigned score graphically allows the user to correct the current function f, as well as dynamically alter their intended target function F in response to new or changing information.

In visualizations where the horizontal axis embedding represents the similarity between the data instances, the system could also enable the user to adjust the position of instances along the horizontal axis, thereby allowing the user to correct both the value assigned to an instance as well as its similarity to other instances. In this paper, we assume that the user cannot graphically influence the similarity metric for the data, which is fixed after the time of manifold construction.

Learning the Scoring Function

While the interaction mechanisms provide a means for the user to correct the value assigned to a single instance, it would be cumbersome for the user to adjust the values of all incorrect instances. Ideally, we want the user to correct the value for as few instances as possible, with the system attributing these adjustments onto the geometry underlying the data in order to learn the scoring function f.

To enable the generalization of each correction to nearby instances, we organize the data onto a manifold that captures the local similarities in the data. The basis functions of this manifold capture the geometry inherent in the data. By learning the scoring function on the manifold rather than the raw data, we can localize each data adjustment to affect only the local neighborhood, rather than the entire data set.

Constructing the manifold

We construct the underlying manifold $\mathcal{M}$ by representing each data instance $\mathbf{x_i} \in X$ as a vertex $v_i \in V$ in a graph $G = (V, \mathbf{A})$. G represents a discrete sample of the continuous manifold $\mathcal{M}$ underlying the data. Each vertex in the graph G is connected to its k-nearest neighbors, according to a radial basis function of the local Euclidean distance between the feature vectors, to form the adjacency matrix $\mathbf{A}$:

$$A_{i,j} = \begin{cases} \exp\left(\frac{-||\mathbf{x_i}-\mathbf{x_j}||^2}{2\sigma^2}\right) & \text{if } v_i \text{ and } v_j \text{ are } \\ & k\text{-nearest-neighbors} \\ 0 & \text{otherwise} \quad . \end{cases} \tag{1}$$

The parameter σ controls the rate at which the affinity falls off with increasing distance. This approach could also be adapted to use other distance metrics besides Euclidean distance, such as the geodesic distance along the manifold as computed by ISOMAP (Tenenbaum, et al. 2000).

Learning functions on the manifold

Once G has been constructed, we construct a set of basis functions on the graph using techniques from spectral graph theory (Chung 1994). These basis functions capture the various components of the graph with respect to its geometry, and are a discrete approximation to the continuous basis functions of $\mathcal{M}$. Using these components, we can represent arbitrary functions on the graph, or take various C-order approximations to those functions with respect to the graph. Using the graph's basis rather than the raw data enables each corrected value to affect the learned model with respect to the geometry underlying the data.

The graph's basis vectors are given as the eigenvectors of the graph's Laplacian (Chung 1994). Let $n = |V|$ and let $\mathbf{D}$ be the degree matrix, formed by $D_{i,i} = \sum_{j=1}^{n} A_{i,j}$. The graph's normalized Laplacian $\boldsymbol{\mathcal{L}}$ is given by the symmetric matrix

$$\boldsymbol{\mathcal{L}} = \mathbf{I} - \mathbf{D}^{-\frac{1}{2}}\mathbf{A}\mathbf{D}^{-\frac{1}{2}} \ , \tag{2}$$

where $\mathbf{I}$ is the identity matrix. Chung (1994) also defines the combinatorial Laplacian $\mathbf{L} = \mathbf{D} - \mathbf{A}$. While both forms of the graph Laplacian are valid, we found that the normalized Laplacian $\boldsymbol{\mathcal{L}}$ yields better results, and so we focus on it for the remainder of this paper.

Taking the eigendecomposition of $\boldsymbol{\mathcal{L}}$ yields $\boldsymbol{\mathcal{L}} = \mathbf{Q}\boldsymbol{\Lambda}\mathbf{Q}^{\mathsf{T}}$, where the columns of $\mathbf{Q} = [\mathbf{q_1} \ldots \mathbf{q_n}]$ are the eigenvectors corresponding to the eigenvalues given in the diagonal matrix $\boldsymbol{\Lambda} = diag(\lambda_1, \ldots, \lambda_n)$. According to spectral graph theory, the eigenvalues $\lambda_1 \ldots \lambda_n$ of $\boldsymbol{\mathcal{L}}$ are real and non-negative. Without loss of generality, we sort the eigenvectors in non-decreasing order of eigenvalue such that $0 = \lambda_1 \leq \lambda_2 \leq \ldots \leq \lambda_n$, where $\mathbf{q_i}$ is the eigenvector corresponding to λ_i. The lowest-order eigenvector $\mathbf{q_1}$ is constant with $\lambda_1 = 0$. The eigenvectors in $\mathbf{Q}$ form an orthonormal basis for $\boldsymbol{\mathcal{L}}$ that respects the graph's geometry.

As stated previously, the graph G represents a discrete approximation of the continuous Riemannian manifold $\mathcal{M}$ with Riemannian metric ψ that underlies the data. Each vertex represents a location on the manifold, with edges weighted based on the distance to its local neighbors. Let $g : \mathcal{M} \to \mathbb{R}$ be a smooth function on the manifold. The Laplace-Beltrami operator Δ is defined to be the divergence of the gradient of $\mathcal{M}$, and can act on any smooth function g defined on $\mathcal{M}$. Hodge theory (Rosenberg 1997) implies that g has a discrete spectrum based on the eigenfunctions of the Laplace-Beltrami operator on $\mathcal{M}$.

The Laplacian $\boldsymbol{\mathcal{L}}$ is a discrete form of the continuous Laplace-Beltrami operator Δ that acts on a smooth function $f : V \to \mathbb{R}$ defined on G:

$$\boldsymbol{\mathcal{L}}f(u) = \frac{1}{\sqrt{d_u}} \sum_{v:v\sim u} \left(\frac{f(u)}{\sqrt{d_u}} - \frac{f(v)}{\sqrt{d_v}} \right) \ , \tag{3}$$

where $v \sim u$ denotes that v is adjacent to u in G, and d_u denotes the degree of u. Like the continuous g, f can also be characterized by $\boldsymbol{\mathcal{L}}$'s eigenfunctions. Therefore, $\mathbf{Q}$ forms a complete orthonormal basis that can be used to define f.

Using the eigenvector basis, we can write the function $f : V \to \mathbb{R}$ as $\mathbf{f} = \mathbf{QW}$, where $\mathbf{f}$ is an $n \times 1$ vector specifying the current value for each vertex, and $\mathbf{W}$ is some $n \times 1$ vector of weights over the eigenvectors. The vector $\mathbf{f}$ specifies the score for each vertex, with corrected instances having the user-specified value, and the scores of the remaining instances assigned by the initial scoring function $\tilde{F}$.

We fit $\mathbf{W}$ using weighted least squares on the eigenvector basis $\mathbf{Q}$ and the values assigned to each instance. In order to focus the fit on the lower order eigenvectors (i.e., the low-frequency components of the graph), we regularize the least squares fit of each eigenvector by the corresponding eigenvalue. Lower order components receive little regularization due to their small eigenvalues, while higher order components are increasingly regularized. This approach provides a "one-shot" method of regularizing the learned function, instead of trying various C-order approximations to $\mathbf{Q}$, and constrains the smoothness of the learned function. From our experience, this approach provides good performance (only slightly higher error than a fitted C-order approximation of $\mathbf{Q}$) at substantially reduced computational cost, which is essential for the interactive nature of this application.

Given $\mathbf{Q}$ and $\mathbf{f}$, the column-vector $\mathbf{W}$ can be fit using regularized weighted least squares by solving the following optimization problem:

$$\mathbf{W} = \arg_{\mathbf{w}} \min \sum_{i=1}^{n} \Omega_{i,i}(f_i - \mathbf{Q_{i,*}}\mathbf{w}) + ||\sqrt{\boldsymbol{\Lambda}}\mathbf{w}||^2 \ , \tag{4}$$

where $\boldsymbol{\Omega}$ is an $n \times n$ diagonal matrix that specifies the weight of each instance, enabling us to ascribe higher weight to those points that are adjusted by the user (as discussed below), $\mathbf{Q_{i,*}}$ is the ith row of $\mathbf{Q}$, and $\sqrt{\boldsymbol{\Lambda}}$ serves as the regularization operator in this Tikhonov regularization problem (Wahba 1990; Tikhonov and Arsenin 1977). The regularization term $||\sqrt{\boldsymbol{\Lambda}}\mathbf{w}||^2$ acts as a weighted penalty on the function's average second-derivative, enforcing smoothness by scaling each eigenvector's weight by its corresponding eigenvalue λ_i, thereby increasing the regularization on higher order eigenvectors (those with larger eigenvalues) to prevent overfitting with the high-frequency components. This technique has been previously used in the context of knowledge transfer by Eaton et al. (2008).

The regularization operator $\sqrt{\boldsymbol{\Lambda}}$ is derived by constraining the smoothness of f (i.e., the L2 norm of the gradient of f) given by: $\langle \nabla \mathbf{f}, \nabla \mathbf{f} \rangle = \langle \mathbf{f}, \boldsymbol{\mathcal{L}}\mathbf{f} \rangle = (\mathbf{Qw})^{\mathsf{T}}(\boldsymbol{\mathcal{L}}\mathbf{Qw}) = \mathbf{w}^{\mathsf{T}}\mathbf{Q}^{\mathsf{T}}(\mathbf{Q}\boldsymbol{\Lambda}\mathbf{Q}^{\mathsf{T}}\mathbf{Qw}) = \mathbf{w}^{\mathsf{T}}\mathbf{I}\boldsymbol{\Lambda}\mathbf{I}\mathbf{w} = \mathbf{w}^{\mathsf{T}}\boldsymbol{\Lambda}\mathbf{w} = ||\sqrt{\boldsymbol{\Lambda}}\mathbf{w}||^2$. Therefore, this learning approach is equivalent to a special case of Belkin et al.'s (2006) Manifold Regularization where the regularization depends only on the smoothness of the learned function f, without a penalty on the magnitude of the solution.

Solving Equation 4 yields the optimal $n \times 1$ weight vector

$$\mathbf{W} = \left(\mathbf{Q}^{\mathsf{T}}\boldsymbol{\Omega}\mathbf{Q} + \boldsymbol{\Lambda}\right)^{-1} \mathbf{Q}^{\mathsf{T}}\boldsymbol{\Omega}\mathbf{f} \ . \tag{5}$$

The learned function $\tilde{f} : V \to \mathbb{R}$ is then given by $\tilde{\mathbf{f}} = \mathbf{QW}$, assigning a value $\tilde{f}_i$ to each instance $\mathbf{x_i}$. The function $\tilde{f}$ then becomes f for the next round of correction by the user.

Weighting the corrected instances

In order to focus learning on the instances corrected by the user, we ascribe higher weight to the corrected instances in the least squares fit. The weight of each instance v_i is given by $\Omega_{i,i}$, forming the $n \times n$ diagonal matrix $\boldsymbol{\Omega}$ used in Equations 4 and 5. We set the weights of all unadjusted instances to be equal to 1, and weight all adjusted instances with a scalar $\omega \in [1, \infty)$. The GUI allows the user to vary ω on a log scale via a slider bar, enabling the user to interactively explore the amount of generalization for the adjustments and dynamically view the resulting model as ω varies. Our experiments show that learning using the manifold basis yields stable results as ω varies from 10 to $10,000$ (three orders of magnitude), rendering it unnecessary to precisely fit ω.

Scaling to large volumes of data

Applying this approach to large volumes of data presents a challenge for modeling the graph structure underlying the data and maintaining interaction with the user. The size of the adjacency matrix $\mathbf{A}$ for the underlying graph grows with the square of the number of data instances. Fortunately, $\mathbf{A}$ can be efficiently stored as a symmetric banded matrix, since each data instance is connected to its k nearest neighbors, substantially reducing the storage requirements.[1] The reverse Cuthill-McKee algorithm (1969) can be used to reduce the full $\mathbf{A}$ matrix to a symmetric banded form. The graph Laplacian $\boldsymbol{\mathcal{L}}$ is therefore also a symmetric banded matrix, and its eigendecomposition can be accomplished efficiently using standard sparse eigen-solvers, such as Lanczos methods. This approach was previously used by Shi and Malik (1998) for efficient image clustering.

While this approach enables the efficient construction and storage of the manifold underlying the data, and the efficient computation of its basis vectors, it yields a full matrix $\mathbf{Q}$ of the eigenvectors. Learning the scoring function using a full matrix for $\mathbf{Q}$ incurs a substantial cost, which threatens the interactive nature of the learning. Using a C-order approximation of the matrix $\mathbf{Q}$ (keeping only the C lower order components, corresponding to those eigenvectors with smaller eigenvalues) will reduce the computational cost of learning via Equation 5, but sacrifices the detailed fit afforded by the higher order eigenvectors.

The Nyström approximation (Baker 1977; Fowlkes et al. 2004) enables us to sample the data instances and learn on a portion of the complete manifold. We can then approximate the scoring function at all other data instances. This approach also enables us to extend f to new data instances. Let $\hat{X} \subseteq X$ be a sample of the data instances sufficient to capture $\mathcal{M}$'s underlying structure. Using the procedure described in the previous section, we can construct the graph $\hat{G}$ underlying $\hat{X}$, form a set of basis functions $\hat{\mathbf{Q}} = [\hat{\mathbf{q}}_\mathbf{1} \ldots \hat{\mathbf{q}}_{|\hat{\mathbf{X}}|}]$ over $\hat{G}$ with eigenvalues $\hat{\boldsymbol{\Lambda}} = diag(\hat{\lambda}_1, \ldots, \hat{\lambda}_{|\hat{X}|})$, and learn a function $\hat{\mathbf{f}} = \hat{\mathbf{Q}}\hat{\mathbf{W}}$ on $\hat{G}$ (Equation 5). The Nyström method enables us to extend the basis vectors of $\hat{G}$ and the learned function $\hat{f}$ to the remaining (or new) data instances $X^{\mathsf{c}} = X - \hat{X}$. For a data instance $\mathbf{x} \in X^{\mathsf{c}}$, represented by vertex v, the value of eigenvector $\hat{\mathbf{q}}_\mathbf{i}$ at v is given by

$$\hat{q}_i(v) = \frac{1}{\hat{\lambda}_i |\hat{X}|} \sum_{j=1}^{|\hat{X}|} w_j \hat{q}_i(\hat{v}_j) \ , \tag{6}$$

[1]Note that the band's width may be larger than k since a vertex may be connected to more than k other vertices.

where $\hat{v}_j$ represents instance $\hat{\mathbf{x}}_\mathbf{j} \in \hat{X}$, $\hat{q}_i(\hat{v}_j)$ is the jth value of $\hat{\mathbf{q}}_\mathbf{i}$, and

$$w_j = \begin{cases} \exp\left(\frac{-||\mathbf{x} - \hat{\mathbf{x}}_\mathbf{j}||^2}{2\sigma^2}\right) & \text{if } \hat{\mathbf{x}}_\mathbf{j} \text{ is a } k\text{-nearest-neighbor to } \mathbf{x} \\ 0 & \text{otherwise} \end{cases} .$$

The value of the scoring function for data instance $\mathbf{x}$ is then

$$\hat{f}(\mathbf{x}) = \sum_{i=1}^{|\hat{X}|} \hat{q}_i(v) \hat{W}_i \ . \tag{7}$$

The above procedure will allow the user to adjust the value of any instance included in the sample $\hat{X}$ and have that correction affect the learning of $\hat{\mathbf{f}}$. However, since all instances are displayed to the user in the scatterplot, regardless of whether they are included in the sample, we must also provide a method for users to adjust the value of instances in X^{c}. When a user chooses to adjust an instance in X^{c}, we explicitly add that instance's eigenvector representation (computed via Equation 6) into $\hat{\mathbf{Q}}$ as an additional row, thereby allowing the adjustment to affect the learning of $\hat{\mathbf{f}}$.

Evaluation

Our experiments show that interactive manifold-based learning rapidly corrects the learned function f as compared to several alternative approaches. As the starting model $\tilde{F}$ for learning, we fit a linear regression model to the data, using a ridge parameter of 10E-8 for regularization. Then, a simulated user repeatedly selects the "most incorrect" data instance that has not yet been adjusted and drags that instance to the correct value. The correct values are given by the true target function F, which is specified by the ground truth values in each data set. Users are adept at identifying data that are grossly incorrect, motivating our simulation of a user adjusting the instances in order from highest to lowest error. After each adjustment, the model f is retrained and evaluated against the true target function F.

Table 1 describes the data sets used in the evaluation. The attribute values of each[2] data set were normalized to lie in $[0, 1]$. Since each experiment uses all available data and the learning is deterministic, there is one "most incorrect" adjustment sequence for each algorithm and data set pairing.

Our interactive learning approach uses weighted least squares with Laplacian regularization on the manifold basis to learn f. The data manifold is constructed using $k = 3$ and $\sigma = 1$. We compare interactive learning using the manifold basis to interactive learning using two alternative approaches: support vector regression (SVR) with an RBF kernel ($\gamma = 0.01$), and least squares regularized with a ridge parameter of 10E-8 on the base feature set X (ablating the manifold basis). We used the implementation of these algorithms with their default parameters from the Weka toolkit (Witten and Frank 2005). For each method, we varied the weight ω assigned to adjusted instances from 1 to $1,000$; unadjusted instances have a weight of $\omega = 1$.

[2]With the exception of the Pyrimidines data set, whose attribute values already are in $[0, 1]$.

Name	#Inst	#Dim	Predicted Attr	Source
CPU	209	6	performance	UCI repository (Asuncion and Newman 2007)
Heart Disease	303	13	cholesterol	UCI repository (Asuncion and Newman 2007)
Pharynx	195	10	survival time	Kalbfleisch and Prentice (1980)[3]
Pyrimidines	74	27	binding activity	King et al. (1992)[3]
Sleep	62	7	danger index	StatLib archive
Wisconsin Breast Cancer	194	32	survival time	UCI repository (Asuncion and Newman 2007)

Table 1: Data sets

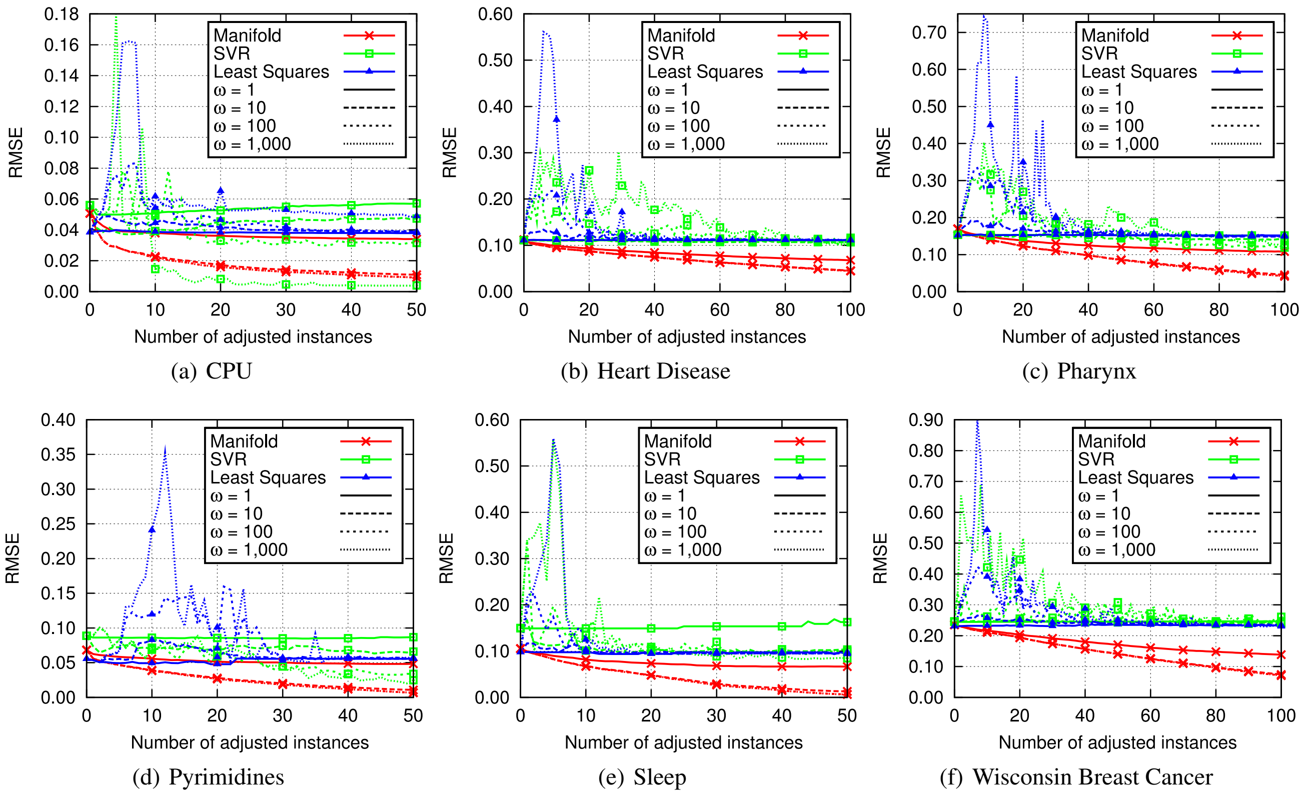

Figure 3: Comparison of interactive learning performance when adjusting the "most-incorrect" instance. We measured the root mean squared error (RMSE) of the three interactive learning methods, each for four values of ω, to the true function F.

As shown in Figure 3, manifold-based interactive learning rapidly reduces the error of the learned model, while the alternative methods are slow to improve performance. With one exception (SVR on CPU after 10 corrections), manifold-based learning achieves better performance than the other methods in all cases. Most importantly, manifold-based learning monotonically reduces the error with each correction. The other methods induce radical jumps in performance with subsequent corrections, often decreasing the model's performance before improving it. From the user's perspective, any decrease in performance (even temporarily) from a correction reduces trust in the learning method. For this reason, the results on all data sets, including CPU, support the use of manifold-based interactive learning over the other approaches. Although it is not visible in Figure 3, the alternative methods do eventually improve performance, but only once most instances have been corrected.

Additionally, our results show that manifold-based interactive learning is stable to perturbations of the weight ω for the corrected instances over three orders of magnitude, from $\omega = 10$ to $\omega = 10,000$. The performance of manifold-based learning with $\omega = 10,000$ was identical to its performance under $\omega = 1,000$ while SVR and least squares displayed even more erratic behavior, and so we omit these results from the graphs for clarity of presentation.

We also conducted a second set of experiments that yield insight into each method's ability to alter the learned model in response to user feedback. In these experiments, instead of correcting the most-incorrect instance, the simulated user corrects random instances (without repetition). Figure 4 shows the results of random correction on the data sets, averaged over 100 trials.

Manifold-based interactive learning is the only method that monotonically improves performance in response to any correction. The other methods first overfit the corrected data,

[3]Also available from the Weka data set collection at http://www.cs.waikato.ac.nz/ml/weka/index_datasets.html

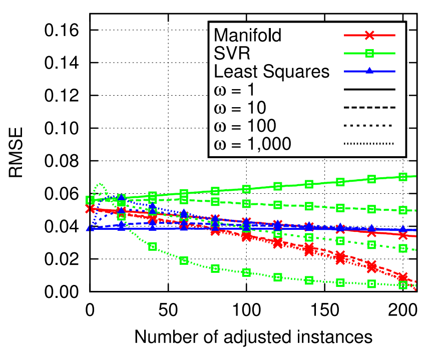

(a) CPU

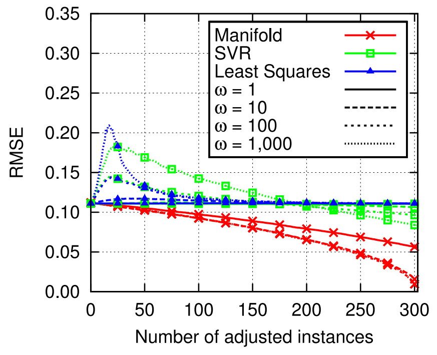

(b) Heart Disease

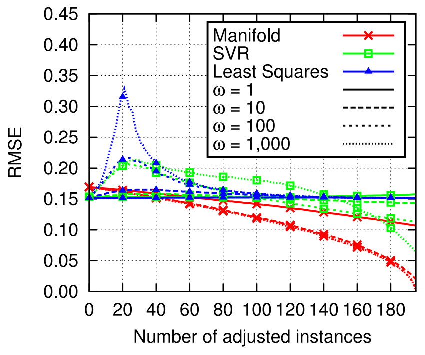

(c) Pharynx

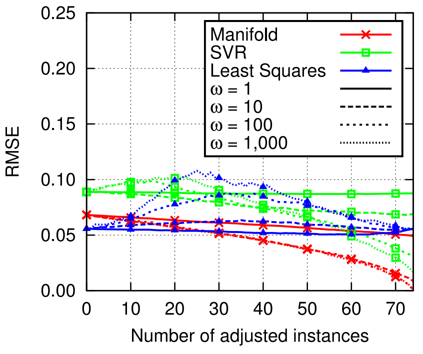

(d) Pyrimidines

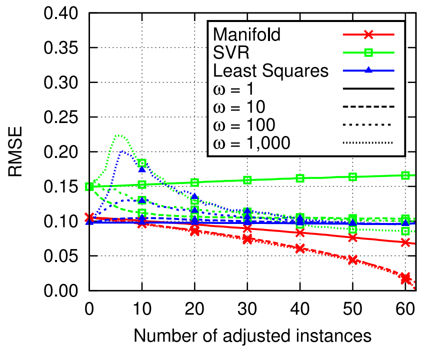

(e) Sleep

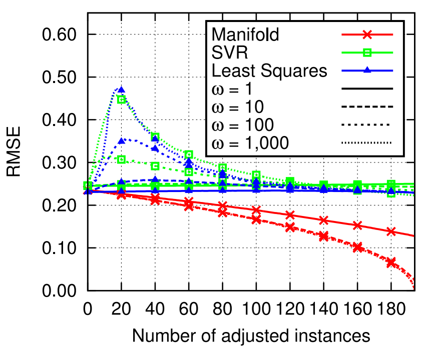

(f) Wisconsin Breast Cancer

Figure 4: Comparison of interactive learning when adjusting a random instances to the correct value, averaged over 100 trials.

decreasing the model's performance, until there are enough corrected instances to avoid overfitting. This experiment reveals the ability of manifold-based interactive learning to temper the effect of any single adjustment, allowing it to have a large impact only if justified by the geometry underlying the data. Additionally, in practical use, the user may not always adjust the most-incorrect instance, as explored in the first experiment. Most likely, an actual user will vary somewhere between these two selection methods (most-incorrect and random), and the results in Figure 4 show that we may expect all user corrections to improve performance under manifold-based interactive learning.

Related Work

The interactive learning framework we have described bears resemblance to active learning, with several important distinctions. Active learning (Cohn, et al. 1996; McCallum and Nigam 1998; Tong 2001) seeks to selectively choose instances for labeling by a "teacher" in order to increase the model's performance using the minimum number of labeled instances. Active learning is driven by automation—the learning algorithm selects the instances for labeling.

In contrast, interactive learning is *user-driven*—the user chooses the adjustments to the model. Interactive learning starts with an initial model and assists the user's exploration of refinements. The initial model may be entirely correct at the time of its creation, but changes in the target concept may reduce its correctness over time; interactive learning provides a means for the user to adjust the model over time and for the system to use each adjustment to the maximum effect. Additionally, active learning starts with unlabeled data and no model; interactive learning starts with unlabeled data and an *incorrect* model. In this manner, interactive learning is complementary to active learning.

Interactive learning is a relatively unexplored branch of machine learning, bridging between automated learning and human-computer interaction. One key dimension of variability in interactive learning approaches is the amount of modeling expertise they require of the user. On one end of the spectrum, users treat the modeling process as a black box and interact only with the model's output; our interactive learning approach belongs in this category. Another example is the interactive classifier by Fails and Olsen (2003) for object recognition in images. In their system, users repeatedly draw rough sketches of objects, and then correct the resulting recognition boundaries based on the metaphor of coloring with crayons. In desJardins et al.'s (2008) interactive visual clustering, users move data instances in a spring-embedding layout to correct the model's output. The system infers constraints based on the user's adjustments, which are then used in constrained clustering to iteratively refine the partitioning.

At the other end of the spectrum, users interact directly with the internals of the model, enabling fine control over the resulting model, but requiring high levels of expertise in modeling. For example, Ware et al.'s (2001) interactive tool for decision tree construction allows the user to control each split in the decision tree; the system visualizes the classification boundaries of each possibility to support the user's choice. Interactive feature selection (Dy and Brodley 2000) and ensemble construction (Talbot et al. 2009) provide the user fine control over other learning steps. The CueFlik system (Fogarty et al. 2008) for image search lies in the middle of the spectrum by allowing users to create individual filtering rules based on training data chosen by the user.

Conclusion

Using the manifold basis enables interactive learning to refine the learned model based on the geometry underlying the data. The results show that this approach improves the performance of the learned model with each correction, unlike alternative approaches. However, we leave a rigorous proof that this method will improve performance with each correction to future work. Our future work will also explore and evaluate methods for handling concept drift and switching target concepts. Additionally, we intend to explore other approaches to incorporating user interaction into learning.

Acknowledgments

This research was supported by internal funding from Lockheed Martin and NSF ITR-0325329. This work is based on methods developed as part of Eric Eaton's dissertation research at the University of Maryland Baltimore County, in collaboration with Marie desJardins and Terran Lane. We thank Sergey Malinchik for discussions on the user interface, and the reviewers for their insightful comments.

References

Asuncion, A., and Newman, D. 2007. University of California Irvine (UCI) machine learning repository. Available at http://www.ics.uci.edu/∼mlearn/MLRepository.html.

Baker, C. T. H. 1977. *The Numerical Treatment of Integral Equations*. Oxford: Clarendon Press.

Belkin, M.; Niyogi, P.; and Sindhwani, V. 2006. Manifold regularization: A geometric framework for learning from labeled and unlabeled examples. *Journal of Artificial Intelligence Research* 7:2399–2434.

Chung, F. R. K. 1994. *Spectral Graph Theory*. Number 92 in CBMS Regional Conference Series in Mathematics. Providence, RI: American Mathematical Society.

Cohn, D. A.; Ghahramani, Z.; and Jordan, M. I. 1996. Active learning with statistical models. *Journal of Artificial Intelligence Research* 4:129–145.

Cuthill, E., and McKee, J. 1969. Reducing the bandwidth of sparse symmetric matrices. In *Proc. of the 24th National Conference of the ACM*, 157–172. New York, NY: ACM.

desJardins, M.; MacGlashan, J.; and Ferraioli, J. 2008. Interactive visual clustering for relational data. In *Constrained Clustering: Advances in Algorithms, Theory, and Applications*, 329-356. Chapman & Hall.

Dy, J. G., and Brodley, C. E. 2000. Visualization and interactive feature selection for unsupervised data. In *Proc. of the 6th ACM SIGKDD International Conference on Knowledge Discovery and Data Mining*, 360–364. ACM Press.

Eaton, E.; desJardins, M.; and Lane, T. 2008. Modeling transfer relationships between learning tasks for improved inductive transfer. In *Proc. of the 19th European Conference on Machine Learning*, 317–332. Springer-Verlag.

Fails, J. A., and Olsen, Jr., D. R. 2003. Interactive machine learning. In *Proc. of the 8th International Conference on Intelligent User Interfaces*, 39–45. ACM Press.

Fogarty, J., Tan, D. S., Kapoor, A., and Winder, S. 2008. CueFlik: Interactive concept learning in image search In *Proc. of the 26th SIGCHI Conference on Human Factors in Computing Systems*, 29–38. ACM Press.

Fowlkes, C.; Belongie, S.; Chung, F.; and Malik, J. 2004. Spectral grouping using the Nyström method. *IEEE Transactions on Pattern Analysis and Machine Intelligence* 26(2):214–225.

Kalbfleisch, J. D., and Prentice, R. L. 1980. *The Statistical Analysis of Failure Time Data*. John Wiley & Sons.

King, R. D.; Muggleton, S.; Lewis, R. A.; and Sternberg, M. J. 1992. Drug design by machine learning. *Proc. of the National Academy of Science U.S.A.* 89(23):11322–11326.

McCallum, A., and Nigam, K. 1998. Employing EM in pool-based active learning for text classification. In *Proc. of 15th International Conference on Machine Learning*, 359–367. San Francisco, CA: Morgan Kaufmann.

Rosenberg, S. 1997. *The Laplacian on a Riemannian Manifold*. Cambridge University Press.

Shi, J., and Malik, J. 1998. Motion segmentation and tracking using normalized cuts. In *Proc. of the 6th International Conference on Computer Vision*, 1154–1160. IEEE Press.

StatLib archive. http://lib.stat.cmu.edu/datasets/.

Talbot, J., Lee, B., Kapoor, A., and Tan, D. S. 2009. EnsembleMatrix: Interactive visualization to support machine learning with multiple classifiers In *Proc. of the 27th SIGCHI Conference on Human Factors in Computing Systems*, 1283–1292. ACM Press.

Tenenbaum, J. B.; de Silva, V.; and Langford, J. C. 2000. A global geometric framework for nonlinear dimensionality reduction. *Science* 290(5500):2319–2323.

Tikhonov, A., and Arsenin, V. 1977. *Solution of Ill-posed Problems*. Winston & Sons.

Tong, S. 2001. *Active Learning: Theory and Applications*. Ph.D. Dissertation, Stanford University.

Wahba, G. 1990. *Spline Models for Observational Data*. Number 59 of CBMS-NSF Regional Conference Series in Applied Mathematics. SIAM.

Ware, M.; Frank, E.; Holmes, G.; Hall, M.; and Witten, I. H. 2001. Interactive machine learning: Letting users build classifiers. *International Journal of Human Computer Studies* 55(3):281–292.

Witten, I. H., and Frank, E. 2005. *Data Mining: Practical Machine Learning Tools and Techniques*, 2nd Edition. San Francisco, CA: Morgan Kaufmann.